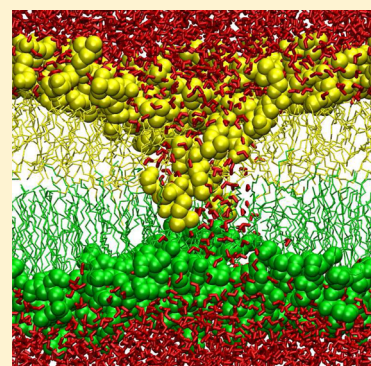


# Electroporation of Asymmetric Phospholipid Membranes

Andrey A. Gurtovenko<sup>\*,†,‡</sup> and Anastasia S. Lyulina<sup>§</sup><sup>†</sup>Institute of Macromolecular Compounds, Russian Academy of Sciences, Bolshoi Prospect V.O. 31, St. Petersburg, 199004 Russia<sup>‡</sup>Faculty of Physics, St. Petersburg State University, Ulyanovskaya str. 1, Petrodvorets, St. Petersburg, 198504 Russia<sup>§</sup>Institute of Physics, Nanotechnology and Telecommunications, St. Petersburg State Polytechnical University, Polytechnicheskaya str. 29, St. Petersburg, 195251 Russia

**ABSTRACT:** As plasma membranes of animal cells are known to be asymmetric, the transmembrane lipid asymmetry, being essential for many membranes' properties and functions, should be properly accounted for in model membrane systems. In this paper, we employ atomic-scale molecular dynamics simulations to explore electroporation phenomena in asymmetric model membranes comprised of phosphatidylcholine (PC) and phosphatidylethanolamine (PE) lipid monolayers that mimic the outer and inner leaflets of plasma membranes, respectively. Our findings clearly demonstrate that the molecular mechanism of electroporation in asymmetric phospholipid membranes differs considerably from the picture observed for their single-component symmetric counterparts: The initial stages of electric-field-induced formation of a water-filled pore turn out to be asymmetric and occur mainly on the PC side of the PC/PE membrane. In particular, water molecules penetrate in the membrane interior mostly from the PC side, and the reorientation of lipid head groups, being crucial for stabilizing the hydrophilic pore, also takes place in the PC leaflet. In contrast, the PE lipid head groups do not enter the central region of the membrane until the water pore becomes rather large and partly stabilized by PC head groups. Such behavior implies that the PE leaflet is considerably more robust against an electric field most likely due to interlipid hydrogen bonding. We also show that an electric field induces asymmetric changes in the lateral pressure profile of PC/PE membranes, decreasing the cohesion between lipid molecules predominantly in the PC membrane leaflet. Overall, our simulations provide compelling evidence that the transmembrane lipid asymmetry can be essential for understanding electroporation phenomena in living cells.



## 1. INTRODUCTION

Trafficking across cell membranes lies at the heart of many biomedical and biotechnological applications, as it is closely related to the delivery of therapeutic molecules to the site of their action. It is therefore essential to have means for manipulating the permeability of cell membranes. One of the widely used approaches for membrane permeabilization is in application of an external electric field to cell membranes (electroporation).<sup>1</sup>

Although the phenomenon is called electroporation, formation of transient hydrophilic pores in membranes upon application of an external electric field remained a hypothesis for many years,<sup>2</sup> as most experimental techniques were unable to provide direct evidence of the pore formation. The molecular-level insight into the pore formation process was unlocked only 10 years ago with the use of atomistic molecular dynamics (MD) simulations.<sup>3,4</sup> Since then, the membrane electroporation has attracted a great deal of attention among computational scientists; see, e.g., refs 5 and 6 for recent reviews.

Historically, electroporation involved relatively long low-magnitude pulses (with the duration of up to milliseconds); such pulses could promote molecular transport mostly across plasma membranes and did not affect the interior of the cell.<sup>7</sup> Recently, the so-called supra-electroporation that employs nanosecond-scale pulses of large magnitude has emerged,<sup>8</sup> so

that electric-field-induced permeabilization of organelle membranes has now become possible.<sup>9</sup>

In MD simulation studies, an electric field is applied to a lipid membrane either as an external force added to all charged atoms in the system<sup>3,4,10–12</sup> or through a transmembrane ionic charge imbalance. The latter cannot be implemented in MD simulations in a straightforward manner due to periodic boundary conditions and requires either two bilayers in a simulation box<sup>13–16</sup> or vacuum slabs<sup>17–19</sup> to prevent ions from jumping across a box. It is believed that direct application of an external electric field to a lipid bilayer system is related to supra-electroporation while applying a transmembrane charge imbalance mimics conventional electroporation when relatively long, low-magnitude pulses make electric charges accumulate at the membrane surface.<sup>18</sup> However, it should be emphasized that such an ion flow (or a “membrane charging”) is not modeled directly in simulations: The charge imbalance is created in the beginning of a simulation run. Furthermore, to witness formation of a pore on time scales accessible through atomistic MD simulations, one needs to create a relatively large ionic charge imbalance so that the induced field strength becomes very close to that observed under direct application of

Received: March 21, 2014

Revised: June 17, 2014

Published: July 1, 2014



an external electric field. It is therefore not surprising that the molecular mechanism of pore formation in zwitterionic lipid membranes was repeatedly demonstrated to be qualitatively similar in both cases, supporting thereby its generic nature.<sup>5,18</sup> In particular, it was shown that the pore formation process is largely driven by the appearance and growth of a water defect spanning the membrane,<sup>4,11,20</sup> which is finalized by a considerable reorientation of lipid head groups toward the membrane interior.<sup>4,10,12</sup> Such hydrophilic pores were proved to serve as permeation pathways for ions<sup>21</sup> and nuclear acids.<sup>10,22</sup> It is noteworthy that after the pore has been formed one witnesses different scenarios that depend on a particular way of application of an electric field. In bilayer systems with an ionic charge imbalance, the growth of a pore is limited by the pore size that allows leakage of ions: Such leakage discharges the transmembrane voltage, and the size of a pore drops.<sup>13–15</sup> In contrast, when an electric field is applied directly to the membrane, the pore continues to expand until the bilayer is ruptured due to the artifacts related to a combined use of periodic boundary conditions and the PME method.<sup>12</sup> To overcome this, one needs to considerably decrease an external electric field once the pore is formed.<sup>12,23</sup>

Most computational studies by far have focused mainly on electroporation of single-component phospholipid bilayers which are usually considered as model systems for mimicking the structural properties of plasma membranes. There are a few exceptions, though: Several groups reported electroporation phenomena in mixed bilayers.<sup>24–28</sup> These studies are highly relevant, as plasma membranes are essentially multicomponent structures. In particular, it was shown that the electroporation threshold of cholesterol-containing phospholipid bilayers exceeds considerably the threshold of their cholesterol-free counterparts due to elevated membrane cohesion.<sup>24,26</sup> Electroporation of mixed phosphatidylcholine/phosphatidylserine lipid membranes was studied in ref 25. The authors found that anionic phosphatidylserine lipids as well as calcium ions bound to the membrane surface inhibit formation of an electropore. Mixed archaeal lipid membranes were studied in ref 27; these membranes were comprised of lipids with relatively massive head groups that contained either inositol or glucose moieties. It was shown that the electroporation threshold of the archaeal lipid membranes is much larger as compared to that measured for phospholipid membranes. Furthermore, adding phosphatidylcholine lipids to the archaeal lipid membrane results in a decrease of their robustness against the electric field.<sup>27</sup> Finally, Reigada reported electroporation of heterogeneous lipid membranes composed of ordered and disordered lipid phases and showed that an external electric field mostly affects the disordered domains.<sup>28</sup>

While the presence of lipid molecules of various types is essential, the plasma membranes of animal cells are also known to be asymmetric as far as the lipid composition of the two opposite leaflets is concerned.<sup>29,30</sup> Such transmembrane lipid asymmetry plays a vital role for many properties and functions of plasma membranes including mechanical stability of membranes<sup>31</sup> and programmed cell death.<sup>32</sup> It is therefore very likely that the lipid asymmetry can also affect the microscopic details related to the electric-field-induced pore formation.

Despite the importance of the lipid asymmetry, there exists only a very limited number of computational papers which would explicitly address the pore formation in such membranes. In particular, electroporation of phosphatidylcholine (PC) lipid

membranes with asymmetric transmembrane distribution of anionic phosphatidylserine (PS) lipids was studied in refs 16 and 33. The authors demonstrated that application of an electric field to such membranes leads to pore formation followed by transmembrane pore-facilitated translocation of anionic lipids. Although not being directly related to the plasma membranes of animal cells, it is also worth mentioning the study by Khalid et al.<sup>34</sup> who explored electroporation phenomena in multicomponent asymmetric bacterial membranes.

To the best of our knowledge, the above-mentioned publications are the only computational studies of electric-field-induced effects in asymmetric biomembranes. Therefore, the main objective of our present work is to meet a lack of such studies. For doing that, we have carried out extensive atomic-scale MD simulations of electroporation in asymmetric phospholipid membranes that are comprised of phosphatidylcholine (PC) and phosphatidylethanolamine (PE) lipid monolayers. The PC and PE lipids are predominant zwitterionic phospholipids in the outer and inner leaflets of cell membranes, respectively,<sup>30</sup> so that the asymmetric PC/PE lipid membranes considered mimic the lipid composition of plasma membranes. As mentioned above, a particular way of application of an electric field leads to qualitatively similar molecular mechanisms of electroporation as far as zwitterionic phospholipid membranes are concerned.<sup>5</sup> Here we chose to employ direct application of an external electric field to a membrane system.

Overall, our simulations provide compelling evidence that the molecular mechanism of electric-field-induced pore formation in asymmetric phospholipid membranes differs from that observed for single-component symmetric membranes. Under an external electric field, the PC leaflet of an asymmetric PC/PE membrane turns out to be more prone to water defect formation compared to the PE leaflet. This results in pore formation driven mostly by rearrangement of lipids on the PC side of the membrane. We also show that an electric field induces asymmetric changes in the lateral pressure profile of the asymmetric PC/PE membrane, decreasing the cohesion between lipid molecules predominantly in the PC membrane leaflet.

## 2. METHODS

We have performed atomic-scale molecular dynamics simulations of symmetric single-component (palmitoyl-oleoyl-phosphatidylcholine (POPC) and palmitoyl-oleoyl-phosphatidylethanolamine (POPE)) lipid membranes and asymmetric lipid membranes comprised of POPC and POPE monolayers. An external electric field was applied perpendicular to the membranes' surface; its strength was varied from 0.33 to 0.90 V/nm, depending on the type of membrane system in question. All the considered systems are listed in Table 1. The initial structures of symmetric POPC and POPE lipid bilayers were taken from ref 35 and consisted of 128 lipids and 5088 water molecules. In turn, an asymmetric PC–PE membrane consisted of 51 lipids on the POPC side and 64 lipids on the POPE side and was solvated with 5147 water molecules; the asymmetric membrane structure was taken from our previous studies.<sup>36–38</sup>

POPC and POPE lipids were described in the framework of an extensively validated united-atom force field by Berger et al.<sup>39</sup> Water was represented by the simple point charge (SPC) model.<sup>40</sup> The Lennard-Jones interactions were cut off at 1 nm, and the electrostatic interactions were handled with the use of

Table 1. Simulated Lipid Membrane Systems

membrane system	applied electric field (V/nm)	voltage <sup>a</sup> (V)	poration time <sup>b</sup> (ns)
POPC-0.0	0	0	no pore (500 ns)
POPC-0.33	0.33	2.37	no pore (200 ns)
POPC-0.40	0.40	2.84	13.66 ± 2.23
POPC-0.45	0.45	3.25	6.72 ± 1.82
POPC-0.50	0.50	3.62	3.77 ± 1.11
POPC-0.60	0.60	4.37	1.07 ± 0.42
POPC-0.70	0.70	5.09	0.68 ± 0.16
POPE-0.0	0	0	no pore (500 ns)
POPE-0.33	0.33	3.11	no pore (200 ns)
POPE-0.40	0.40	3.71	no pore (200 ns)
POPE-0.45	0.45	4.14	no pore (200 ns)
POPE-0.50	0.50	4.5	no pore (200 ns)
POPE-0.60	0.60	5.28	44.64 ± 15.63
POPE-0.70	0.70	6.12	13.83 ± 5.54
POPE-0.80	0.80	7.16	3.15 ± 0.85
POPE-0.90	0.90	8.05	0.95 ± 0.11
PC/PE-0.0	0	0	no pore (500 ns)
PC/PE-0.40	0.40	3.45	no pore (500 ns)
PC/PE-0.45	0.45	3.9	37.85 ± 9.88
PC/PE-0.50	0.50	4.33	11.46 ± 1.86
PC/PE-0.50M <sup>c</sup>	-0.50	-4.31	12.35 ± 2.81
PC/PE-0.60	0.60	5.22	2.90 ± 0.55

<sup>a</sup>A voltage developed in a membrane system upon application of an external electric field  $E$ . The voltage was calculated as  $V = EL_z$ , where  $L_z$  is the average size of a simulation box in the direction of the applied field.<sup>10,49–51</sup> <sup>b</sup>Poration times are calculated by averaging over five independent simulation runs; all five runs in a series have resulted in pore formation. The errors presented are standard errors of the mean. <sup>c</sup>An external electric field with a reversed polarity.

the particle-mesh Ewald method (PME).<sup>41</sup> All systems were simulated in the  $NpT$  ensemble at the physiological temperature ( $T = 310$  K) and at a pressure set to 1 bar. The velocity-rescaling thermostat<sup>42</sup> was used for controlling temperature in the system. We used the Parrinello–Rahman scheme<sup>43</sup> to control pressure; the pressure coupling was applied semi-isotropically, i.e., independently for the extension of a simulation box in the direction of the bilayer normal and for the cross-sectional area of the box in the plane parallel to the membrane surface. The time step used was 2 fs. The simulations of the membrane systems with no pore formed were carried out over a period of 200 ns with the exception of POPC-0.0, POPE-0.0, PC/PE-0.0, and PC/PE-0.40 systems for which the simulations were extended up to 500 ns. For each porated membrane system, the simulations were repeated five times with different initial conditions. All in all, we have performed MD simulations of 74 membrane systems. The combined simulated time amounts to 4.6  $\mu$ s. The GROMACS suite was used in all of the simulations.<sup>44,45</sup>

To characterize mechanical properties of lipid membranes, we evaluated the lateral pressure profile across a membrane (along the membrane normal  $Z$ ). For doing that, we employed a recent approach to calculate local stress in biomembranes;<sup>46</sup> this method uses the central force decomposition and also accounts for constraints. In practice, simulations of four membrane systems (POPC-0.0, POPE-0.0, PC/PE-0.0, and PC/PE-0.40) were extended for 200 ns each (in addition to 0.5  $\mu$ s runs that were considered as pre-equilibration). During these additional runs, the positions and velocities were stored every 10 ps, resulting in 20 000 frames for each system. These

simulation frames were employed then for calculating the local stress profile with the use of the custom Gromacs-4.5 version,<sup>46</sup> which relies heavily on a previous Gromacs-based local pressure code.<sup>47</sup>

### 3. RESULTS

**A. Electroporation of Symmetric Phospholipid Membranes.** We start by considering electroporation phenomena in symmetric single-component phospholipid membranes. The two most abundant types of zwitterionic lipids, phosphatidylcholine (PC) and phosphatidylethanolamine (PE), were chosen for our simulation study. The former is a typical representative of the outer leaflet of plasma membranes, and the latter is located mostly in the inner leaflet. The major difference of the two lipid types is in the chemical structure of their head groups: PE lipids have primary amines in the head groups, while PC lipids have choline moieties. Because of the amine groups, PE lipids are capable for the formation of intra- and intermolecular hydrogen bonds.<sup>48</sup> This results in a considerably more densely packed water–lipid interface of a PE membrane as compared to that of a PC counterpart. Therefore, one could anticipate that these two types of lipid membranes will respond differently to an external electric field.

The main results of MD simulations of symmetric PC and PE lipid bilayers under an external electric field are summarized in Figure 1 and Table 1. Besides the electric field applied, we also showed a corresponding voltage  $V$  developed in the

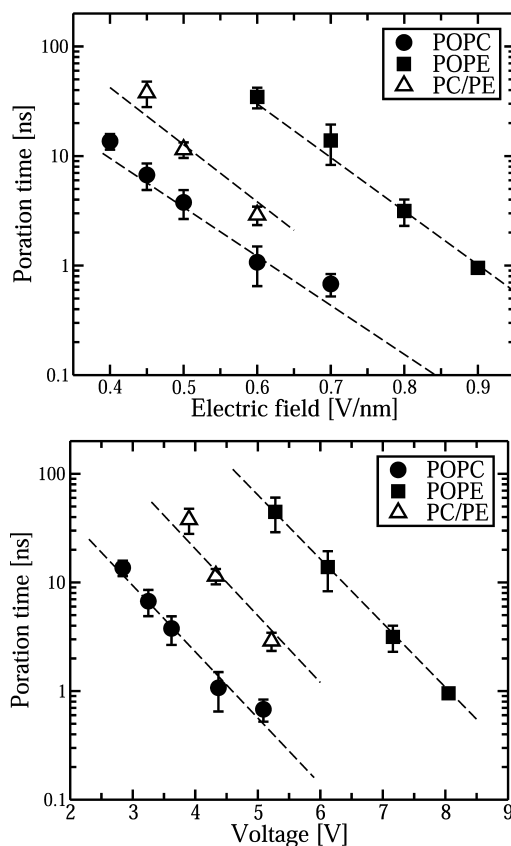


**Figure 1.** Poration time as a function of the applied electric field (top) and the voltage developed in the membrane system (bottom). Shown are the results for POPC (solid circles), POPE (solid squares), and asymmetric PC/PE (open triangles) lipid membranes (semilog scale). The errors are standard errors of the mean.

membrane systems. The latter depends on the average size of a box  $L_z$  along the direction of the applied field  $E_z$  and is defined as  $V = E_z L_z$ , as pointed out in refs 10, 49, 50, and 51.

For symmetric bilayers comprised of palmitoyl-oleoyl-phosphatidylcholine (POPC) lipids, the strength of the applied electric field was varied from 0.33 to 0.70 V/nm (which corresponds to a voltage range from 2.37 to 5.09 V). Only one system, POPC-0.33, shows no pore formation over a period of 200 ns; see Table 1. For the rest of the POPC bilayer systems, the average poration time ranges from 13.66 ns ( $E = 0.40$  V/nm) to 0.68 ns ( $E = 0.70$  V/nm); the poration times are calculated by averaging over five independent simulation runs with different initial conditions (all five simulation runs have ended up with pore formation). As seen in Figure 1, the poration time drops exponentially with the strength of an applied electric field in agreement with earlier observations.<sup>14</sup> The same also holds for the dependence of the poration time on voltage.

As far as PE lipid membranes are concerned, they turned out to be much more robust against an external electric field: We did not witness any pore formation in the bilayers comprised of palmitoyl-oleoyl-phosphatidylethanolamine (POPE) lipids when the applied field was varied from 0.33 to 0.50 V/nm (which corresponds to a voltage range from 3.11 to 4.5 V); see Table 1. Poration was observed in POPE membranes under an electric field of 0.60 V/nm and stronger; the corresponding poration time ranged from 44.64 ns (0.60 V/nm) to 0.95 ns (0.90 V/nm). Again, the poration time follows the same pattern as that for POPC membranes; see Figure 1. Interestingly, the slopes of exponential fits of the “poration time–electric field” and “poration time–voltage” curves seem to be almost identical for POPC and POPE lipid membranes.

The relative robustness of POPE lipid membranes to electroporation as compared to POPC membranes is most likely related to the intermolecular hydrogen bonds formed in PE membranes. These interactions lead to a denser packed water–lipid interface and to more ordered hydrocarbon lipid chains.<sup>35</sup> In particular, the denser water–lipid interface prevents formation of water defects in PE membranes, which is an essential condition for electroporation: Our previous MD simulation studies indeed showed that water permeates deeper into the PC membranes as compared to their PE counterparts.<sup>35</sup>

To further characterize the difference in the water–lipid interface of the PC and PE lipid membranes, we calculated their lateral pressure profiles; see Figure 2. Note that the particular shape of the lateral pressure curves depends on both the method of calculation and the lipid force field employed.<sup>52</sup> Our lateral pressure profile of a POPC bilayer practically coincides with the corresponding profile reported in ref 46 where the same method and the same lipid force field were used, justifying thereby calculations presented here.

Comparison of the two lateral pressure profiles presented in Figure 2 shows that a PE bilayer is characterized by much deeper minima in the lateral pressure at the lipid–water interface as compared to a PC bilayer, indicating stronger cohesion of PE lipids. What is more, the lateral pressure profile of a PE bilayer has an additional minimum beyond the position of phosphate groups (closer to the water phase); see Figure 2. Such a pronounced minimum is not seen in the case of a POPC bilayer and can be a signature of attractive interactions resulting from hydrogen bonds between POPE lipids (we note that the lateral pressure profile of a PE bilayer turns out to not be

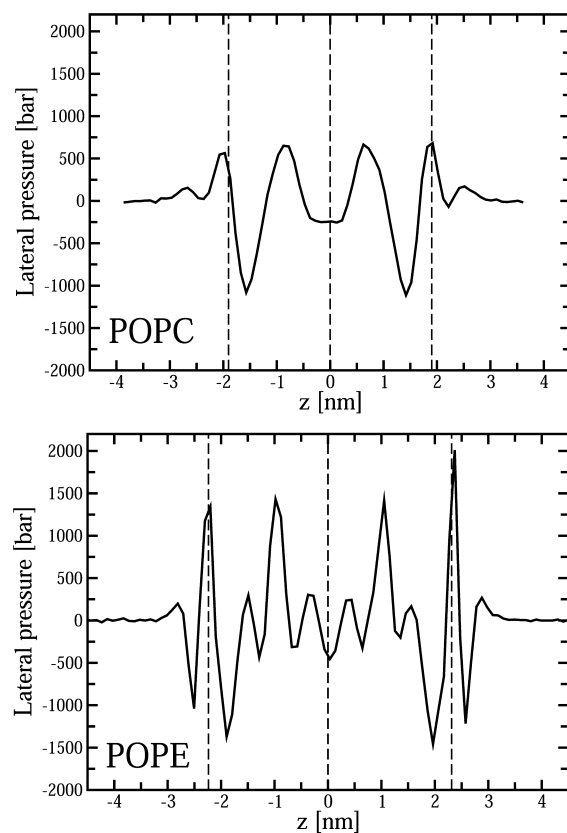


**Figure 2.** Lateral pressure profiles for POPC (top) and POPE (bottom) lipid membranes along the  $z$ -axis (membrane normal). Vertical dashed lines correspond to the membrane center and to the phosphate positions in the opposite leaflets as identified from the corresponding density profiles.

entirely symmetric, indicating that 200 ns might not be sufficient for a full sampling of the profile).

Despite the difference in robustness of PC and PE lipid membranes to an electric field, it turns out that this does not affect the molecular mechanism of pore formation. As an illustration, in Figure 3, we present formation of a water pore in POPC and POPE lipid membranes as induced by an external electric field of 0.60 V/nm. The corresponding voltage applied to the systems equals 4.37 and 5.28 V for POPC and POPE membranes, respectively. In both cases, the process of pore formation begins with a perturbation of the water/lipid interface accompanied by the appearance of a single water defect spanning the entire membrane; see Figure 3. This line of water molecules is normally identified as an intermediate pore state.<sup>12</sup> Remarkably, for both types of symmetric lipid membranes, we did not notice any preference of one leaflet over another as far as initiation of the membrane-spanning water file is concerned. In other words, the initial stages of pore formations in symmetric PC and PE lipid membranes occur in both leaflets with (on average) the same probability. We note that for POPC membranes this conclusion agrees with previous simulation results.<sup>11</sup> Formation of the water file in the membrane interior turns out to be an irreversible event in most cases. Once the membrane-spanning water defect is formed, it grows rapidly, leading to reorientation of lipid head groups toward the membrane interior; see Figure 3. Another feature that can be noticed in Figure 3 is that this rotational reorientation of head groups is much slower in the case of

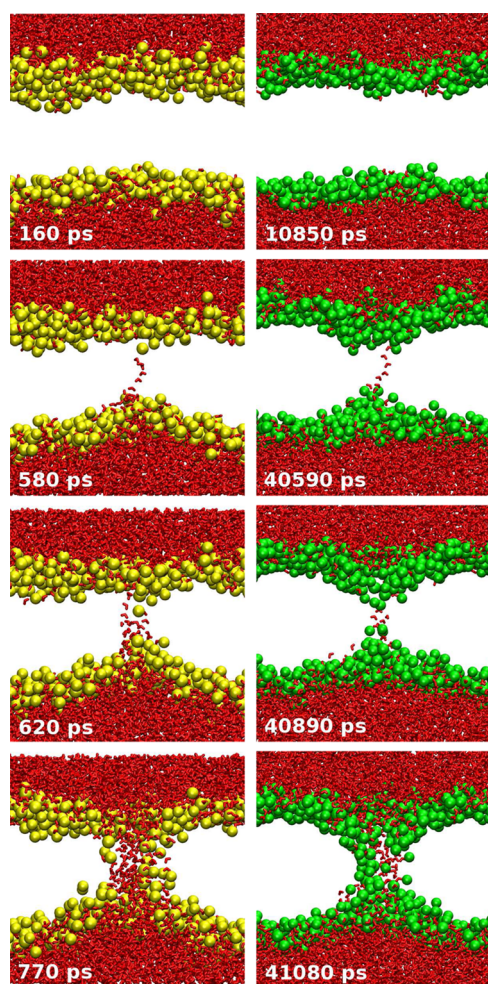


**Figure 3.** Formation of a water pore in symmetric POPC (snapshots on the left-hand side) and POPE (snapshots on the right-hand side) lipid membranes under an external electric field of 0.60 V/nm. The corresponding voltage developed in the systems equals 4.37 and 5.28 V for POPC and POPE membranes, respectively. PC lipid headgroup atoms (nitrogen, phosphorus, and carbonyl oxygens) are shown as yellow spheres, their PE counterparts are shown as green spheres, and the rest of lipid atoms are not shown. Water molecules are shown in red.

POPE lipids. Finally, the polar lipid head groups surround the pore and become its walls, making the pore hydrophilic. All in all, one can conclude that the observed pore formation process follows closely the mechanism reported in previous computational studies for zwitterionic lipid membranes.<sup>3–5,10–12</sup> It is noteworthy that several recent MD studies pointed to the existence of an alternative scenario where water-filled pores can be hydrophobic. Such a situation was observed in cholesterol-rich phospholipid membranes,<sup>26</sup> in anionic phosphatidylserine bilayers,<sup>53</sup> and in archaeal membranes<sup>27</sup> when an ionic charge imbalance was used to trigger electroporation.

Thus, the electroporation threshold differs considerably for single-component POPC and POPE lipid membranes most likely due to hydrogen bonding between PE head groups, resulting in additional cohesive interactions within the POPE lipid–water interface. Despite the fact that POPE membranes require larger poration fields and show longer poration times and slower rotation of lipid head groups as compared to their POPC counterparts, the molecular mechanism of pore

formation stays essentially the same for the two types of phospholipid membranes. This finding is reminiscent of the situation observed for cholesterol-containing membranes where the enhanced robustness of the membranes did not affect the poration mechanism.<sup>24</sup> Furthermore, it is worth mentioning that the electroporation threshold can differ not only due to different chemical structures of lipid head groups but also because of a difference in hydrophobic lipid tails.<sup>54</sup>

To conclude this section, we emphasize that the pore formation process in single-component phospholipid membranes is essentially symmetric with respect to the opposite leaflets. As we will see in the next section, this is not the case for asymmetric membranes.

**B. Electroporation of Asymmetric Phospholipid Membranes.** For studying electroporation phenomena in asymmetric lipid membranes, we chose a model membrane comprised of phosphatidylcholine (PC) and phosphatidylethanolamine (PE) monolayers.<sup>36–38</sup> The PC and PE monolayers of the membrane mimic the extracellular and intracellular leaflets of plasma membranes of eukaryotic cells, respectively.<sup>30</sup>

First of all, poration times measured for asymmetric PC/PE lipid membranes are found to demonstrate intermediate behavior: They are smaller than the corresponding times for symmetric POPE membranes but exceed those for single-component POPC membranes; see Table 1 and Figure 1. What is more, the resistance of an asymmetric membrane to an electric field turns out to not be additive with respect to POPC and POPE monolayers: As is clearly seen for the membrane systems under an electric field of 0.60 V/nm (Figure 1 (top)), the poration time of an asymmetric membrane is considerably closer (on a logarithmic scale) to that of a POPC membrane as compared to its POPE counterpart. In a way, the PC leaflet of an asymmetric PC/PE membrane represents the most vulnerable part of the membrane as far as electric-field-induced poration is concerned. This feature also plays a crucial role in the molecular mechanism of pore formation. Note that the poration times of PC/PE membranes noticeably shift toward the corresponding curve for POPE membranes when plotted as a function of the voltage developed; see Figure 1 (bottom). This is due to the fact that the PE leaflet is thicker than the PC one, increasing thereby the box size  $L_z$  and, correspondingly, the voltage developed in the system.

In Figure 4, we show major steps in electric-field-induced poration of an asymmetric PC/PE lipid membrane under an external electric field of 0.45 V/nm. It is seen that the process of pore formation turns out to be essentially asymmetric with respect to lipid monolayers of different lipid composition: The PC monolayer is much more prone to defect formation as compared to its PE counterpart. In other words, the applied electric field affects mostly the POPC part of the asymmetric membrane, while the POPE part stays almost unperturbed. This is something that one can expect from the MD simulations of one-component symmetric membranes: An electric field of 0.45 V/nm does not porate POPE membranes on a time scale of 200 ns; in contrast, this field leads to pore formation in POPC bilayers within just 10 ns; see Table 1.

Overall, the process of pore formation in asymmetric PC/PE membranes is largely driven by structural changes that occur in the PC leaflet. One witnesses formation of “bumps” in the hydrocarbon region on the PC side, and water molecules also penetrate in the membrane interior mostly from the PC side; see Figure 4. Remarkably, the reorientation of lipid head groups which stabilizes the pore also takes place on the PC side; i.e.,

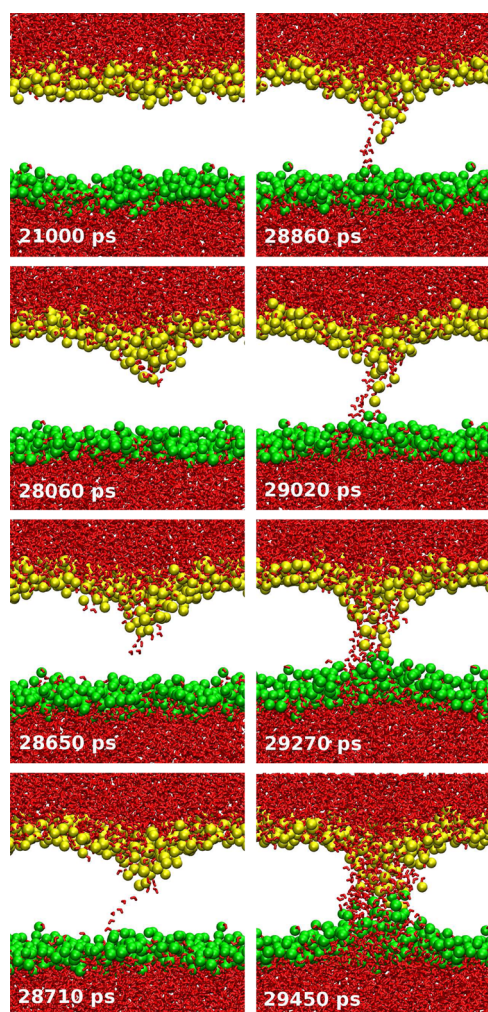


**Figure 4.** Formation of a water pore in an asymmetric POPC/POPE lipid membrane under an external electric field of 0.45 V/nm. Head group atoms of POPC and POPE lipids (nitrogen, phosphorus, and carbonyl oxygens) are shown as yellow and green spheres, respectively. The rest of the lipid atoms are not shown; water is shown in red.

only PC head groups are mainly involved in the early stages of pore formation. Once the pore is formed, PE head groups begin to reorient toward the membrane interior. This can be related in part to much slower rotation of PE lipid head groups, as mentioned in the preceding section.

The overall picture of pore formation in asymmetric membranes turned out to be insensitive to the polarity of an electric field. For a PC/PE membrane under an electric field of 0.50 V/nm (corresponding to a voltage of  $\sim 4.3$  V), we repeated MD simulations with a reverse polarity (Table 1) and did not find any noticeable differences as far as the molecular mechanism of pore formation and the characteristic poration times are concerned. We recall that asymmetric PC/PE membranes possess a nonzero intrinsic transmembrane potential of  $\sim 100$  mV, which is negative on the POPE side.<sup>36–38</sup> Therefore, the observed insensitivity to the field polarity implies that the intrinsic potential of PC/PE membranes has no influence on the electroporation process most likely because the strength of the poration field employed here is more than an order of magnitude larger than the membrane's intrinsic potential; see Table 1.

Interestingly, an electric field of different polarity reorients lipid headgroup dipoles differently. When no field is applied, the average angle between the PN vector of lipids and the outward bilayer normal is found to be 79 and 92° for PC and PE leaflets, respectively. These quantities are very close to those measured for single-component POPC-0.0 and POPE-0.0 membrane systems (78 and 93°); the difference in the PN vector orientation of the two types of lipids is most likely due to hydrogen bonding between PE lipid head groups.<sup>36</sup> When an electric field of 0.50 V/nm is applied to a PC/PE membrane in the PC-to-PE direction, none of the PC and PE head groups are oriented (on average) in the direction of the applied field, so that the corresponding “PN vector–outward bilayer normal” angles change to 82 and 89° for PC and PE leaflets, respectively. In turn, when the polarity of the field changes, i.e., the field is applied in the PE-to-PC direction, both PC and PE lipid head groups tend to align with the field. The corresponding PN angles become 74° (PC) and 95° (PE). Despite such a difference in the response of lipid headgroup dipoles to an electric field of opposite polarity, this does not affect the overall poration mechanism in asymmetric PC/PE membranes.

To further characterize the process of pore formation, we calculated the numbers of water molecules and lipid head groups within a 1.5 nm slab in the middle of the PC/PE membrane shown in Figure 4. The time evolution of these quantities is presented in Figure 5. Again, it is clearly seen that

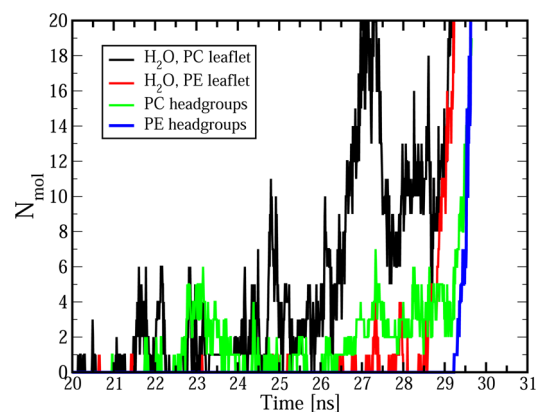


**Figure 5.** Time evolution of numbers of water molecules (shown in black for the PC side and in red for the PE side) and lipid head groups (shown in green for PC lipids and in blue for PE lipids) within a 1.5 nm slab in the middle of the PC/PE membrane under an external electric field of 0.45 V/nm.

the water defects in a pore-free PC/PE membrane (at  $t < 28$  ns) develop mostly in the PC leaflet; see Figure 5. Furthermore, PC lipid head groups can spontaneously appear in the membrane interior to form “bumps”. Interestingly, the curves for the numbers of PC head groups and water molecules on the PC side follow similar patterns at 26.5 ns  $< t < 29$  ns, which can be a signature of the appearance of PC headgroup bumps filled with water. The PE lipid head groups do not show up in the central region of the membrane until the water pore becomes rather large and is stabilized by PC head groups; see Figure 5. After this stage is reached, the PE head groups get reoriented relatively quickly, within just 100–200 ps.

#### 4. DISCUSSION AND CONCLUSIONS

Our findings clearly demonstrate that the molecular mechanisms of electric-field-induced pore formation differ considerably for symmetric and asymmetric phospholipid membranes. Poration of a membrane that is comprised of two monolayers with different robustness against an electric field is driven mostly by formation of structural defects in a less robust lipid monolayer. In a way, our findings are in line with recent MD simulations of laterally heterogeneous lipid membranes<sup>28</sup> where electroporation also occurs mainly in less ordered domains. In the case of the PC/PE membranes considered in this study, the PC side of the membrane becomes more prone to defects induced by an external electric field due to the absence of hydrogen bonding between PC lipid molecules. In contrast to single-component lipid membranes, electroporation of such PC/PE membranes has essentially asymmetric character: Water defects are mainly formed on the PC side of the membrane, and PC head groups play a major role in early stages of pore formation.

The molecular mechanism of pore formation in PC/PE lipid membranes is somewhat similar to the picture reported in ref 34 for *E. coli* outer membranes. One of the monolayers of this bacterial membrane was comprised of phospholipids, while another consisted of lipopolysaccharide (LPS). It was shown that electric-field-induced pore formation was asymmetric and triggered by water defects and lipid headgroup reorientation on the phospholipid side of the *E. coli* outer membrane.<sup>34</sup> This is mostly due to the fact that LPS sugars on one side of the bacterial membrane are much larger than the phospholipid head groups on the opposite side, so that the ability of the LPS sugars to move toward the center of the membrane is very limited. Despite some similarity to the situation found in our work, it has to be emphasized that the observed asymmetric character of electroporation of PC/PE lipid membranes has nothing to do with the relative size of lipid head groups on the opposite membrane sides (one could even notice that PE head groups are somewhat smaller than PC ones). Instead, it is the strength of interlipid interactions that matters most: The hydrogen bonding between PE lipids makes the corresponding leaflet more robust against the applied electric field as compared to the PC leaflet and eventually leads to a pronounced asymmetry in the process of pore formation.

Poration of biological membranes is not the only electric-field-induced effect that has practical importance. As another example, one can mention electro-insertion of proteins into cell membranes.<sup>55</sup> Depending on the type of biomembranes and proteins targeted for insertion, different scenarios can be realized. In particular, the electric-field-induced insertion of proteins can be accompanied by electroporation.<sup>56</sup> However, the electro-insertion does not necessarily require actual pore formation,<sup>57</sup> which is often considered as a damage to cells. To implement such a type of electro-insertion, one needs to employ electric field strengths below the electroporation threshold.<sup>57</sup>

To get insight into the structural changes in asymmetric PC/PE membranes due to an electric field of the strength that is insufficient for poration, we extended MD simulations of PC/PE-0.0 and PC/PE-0.40 membrane systems to half of a microsecond; see Table 1. The electric field of 0.4 V/nm (which corresponds to a voltage of 3.45 V) does not porate a PC/PE membrane on the time scale considered; however, it does affect the structural properties of the membrane. In

particular, the applied electric field has a clear disordering effect on acyl chains in both PC and PE leaflets: The deuterium order parameter for saturated sn-1 acyl lipid chains drops considerably when the electric field is switched on; see Figure 6. A relative decrease is more pronounced on the PE side of the

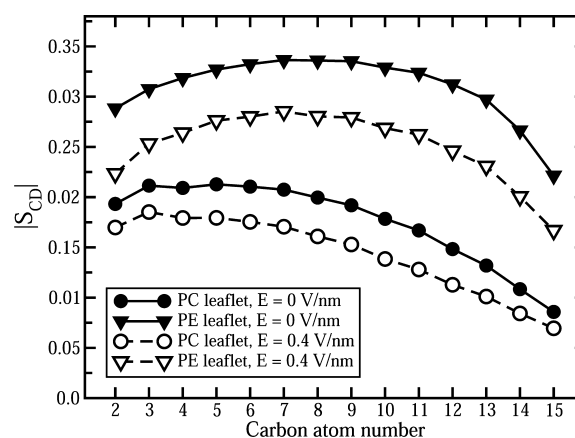


**Figure 6.** Deuterium order parameter  $|S_{CD}|$  for saturated sn-1 acyl chains of POPC (circles) and POPE (triangles) lipids in asymmetric PC/PE membranes. Shown are the results for a membrane system under an electric field of 0.4 V/nm (open symbols) and for a membrane that is not perturbed by an electric field (solid symbols). Low carbon atom numbers correspond to those close to the lipid headgroup.

membrane. However, the lipid tails of the PC leaflet still remain much more disordered as compared to those of the PE monolayer, again rendering the overall situation asymmetric.

As the united-atom Berger force field is used for lipid molecules in this study, the hydrophobic acyl chains do not carry any charges and are not affected directly by an electric field. Furthermore, the electric field is found to have a minor effect on the area per lipid and the membrane thickness (data not shown), so that the observed electric-field-induced disordering of lipid tails cannot be related directly to the changes in these structural membrane characteristics. However, we found a noticeable reorientation of lipid headgroup dipoles. Similar to what was observed for the PC/PE-0.50 system (see previous section), the electric field of 0.4 V/nm applied in the PC-to-PE direction changes the average “PN vector—outward bilayer normal” angle from 79 to 82° on the PC side and from 92 to 87° on the PE side. It is likely that this reorientation of lipid headgroup dipoles is partly responsible for the observed disordering of lipid tails. We note that such a disordering of hydrophobic lipid chains was witnessed in all membrane systems exposed to an external electric field; see Table 1.

To further characterize the electric-field-induced changes, we calculated lateral pressure profiles for asymmetric membrane systems PC/PE-0.0 and PC/PE-0.40; see Figure 7. Interestingly, when no electric field is applied, the lateral pressure profile of a PC/PE membrane represents a combination of halves of the corresponding pressure profiles of single-component PC and PE lipid membranes, see Figure 2, indicating that the opposite leaflets of an asymmetric PC/PE membrane have practically no influence on each other. The same conclusion can be drawn from a comparison of the order parameters and the orientation of headgroup dipoles of PC and PE leaflets of an asymmetric membrane with the corresponding characteristics of symmetric membranes. This is most likely due

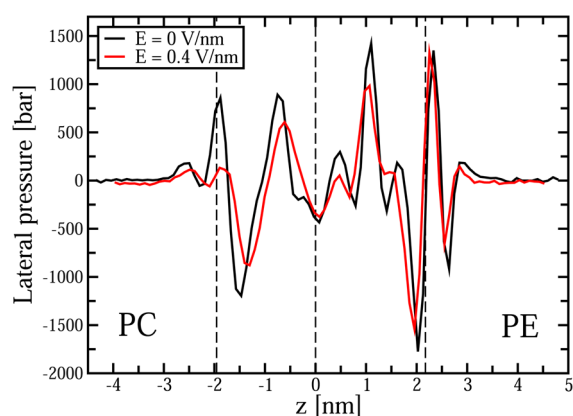


**Figure 7.** Lateral pressure profiles for asymmetric PC/PE lipid membranes with no electric field applied (black line) and with an electric field of 0.4 V/nm (red line). Vertical dashed lines correspond to the membrane center and to the phosphate positions in the opposite leaflets of the PC/PE membrane without an electric field (as identified from the corresponding density profiles).

to the fact that a PC/PE membrane was built in such a way that the equilibrium values of the area per lipid of its monolayers were well preserved; see the Methods section and also ref 36.

Remarkably, when an electric field of 0.4 V/nm is applied to an asymmetric PC/PE lipid membrane, the lateral pressure profile changes asymmetrically. While the PE lipid/water interface stays almost unaffected, the cohesive interactions between PC lipids at the opposite lipid/water interface drop, as seen from the corresponding minimum of the lateral pressure profile on the PC side. Furthermore, the peak in the lateral pressure profile at the PC lipid/water interface vanishes almost completely under the influence of an external electric field. These electric-field-induced changes in the lateral pressure indicate that the PC lipid leaflet becomes more prone to defect formation as compared to its PE counterpart.

This asymmetry can indeed be witnessed through a direct inspection of water defects formed in the opposite leaflets. In Figure 8, we plot the numbers of water molecules  $N_W$  in the inner regions of PC and PE leaflets of asymmetric PC/PE lipid membranes; these quantities can serve as a measure of water defects that are formed in the lipid/water interface on both sides of the membrane. Without an electric field, there is almost no difference between the PC and PE leaflets: The probability to find a water molecule in their hydrophobic interior is very low for both leaflets; see Figure 8 (top). The applied electric field of 0.4 V/nm changes the overall picture drastically, as the PC leaflet now turns out to be more prone to defect formation. As seen in Figure 8 (bottom), water defects on the PC side of the membrane are much larger and occur more frequently as compared to the PE counterpart (we note that, despite the developed defects, a water-filled pore spanning the entire PC/PE membrane is not formed on the time scale considered).

Because the PC monolayer in our model membrane mimics the outer leaflet of the plasma membrane, our findings may be relevant for understanding the molecular mechanism of the above-mentioned electro-insertion techniques used for incorporating relatively large molecules into cell membranes.<sup>57</sup> As we demonstrated, an electric field of a relatively small magnitude can selectively enhance the permeability of the outer (PC) membrane leaflet, affecting the lipid–water interfacial region of its lateral pressure profile and making its lipid tails more disordered. At the same time, the membrane as

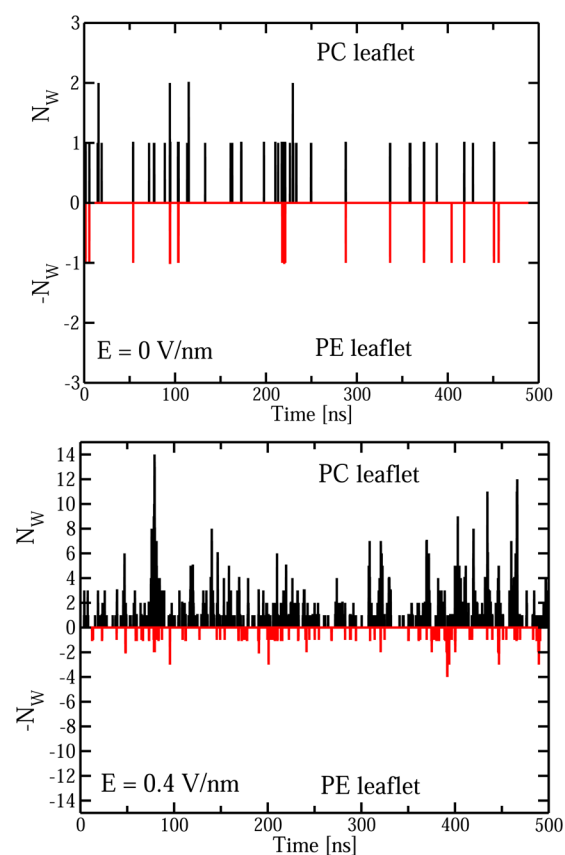


**Figure 8.** Time evolution of numbers of water molecules  $N_W$  within a 1.5 nm slab in the middle of a PC/PE membrane (the values of  $N_W$  are shown in black and red for PC and PE leaflets, respectively). Shown are the results for a membrane that is not perturbed by an external electric field (top) and for a membrane under an electric field of 0.4 V/nm (bottom).

a whole stays intact. These structural changes in the membrane could potentially facilitate insertion of foreign molecules into its outer leaflet. One could also speculate that the electric-field-induced asymmetry in membrane permeability may be relevant to nanoparticle binding to the membrane surface and to subsequent wrapping of a nanoparticle by the bilayer membrane; both of these phenomena are often considered to be essential steps in endocytosis.<sup>58</sup>

To conclude, in this paper, we have employed extensive molecular dynamics simulations to unlock atomic-scale details of electric-field-induced changes in lipid membranes with asymmetric transmembrane lipid composition. We demonstrate that the molecular mechanism of electroporation of asymmetric phospholipid membranes built from phosphatidylcholine and phosphatidylethanolamine leaflets differs considerably from the picture observed for single-component symmetric membranes. In particular, the pore formation process is mainly driven by the phosphatidylcholine side of the membrane, as this leaflet turns out to be more prone to water defect formation under an external electric field. Furthermore, an electric field with a magnitude below electroporation threshold is found to induce asymmetric changes in the lateral pressure profile of an asymmetric PC/PE membrane, decreasing the cohesive interactions between lipid molecules predominantly on the PC side of the membrane.

## ■ AUTHOR INFORMATION

## Corresponding Author

\*E-mail: a.gurtovenko@gmail.com. Web site: biosimu.org.

## Notes

The authors declare no competing financial interest.

## ■ ACKNOWLEDGMENTS

The authors wish to acknowledge use of the computer cluster of the Institute of Macromolecular Compounds RAS and the Lomonosov supercomputer at the Moscow State University.

## ■ REFERENCES

- (1) Neumann, E.; Sowers, A.; Jordan, C., Eds. *Electroporation and Electrofusion in Cell Biology*; Plenum Press: New York, 1989.
- (2) Weaver, J. C. Electroporation of Biological Membranes From Multicellular to Nano Scales. *IEEE Trans. Dielectr. Electr. Insul.* **2003**, *10*, 754–768.
- (3) Tieleman, D. P.; Leontiadou, H.; Mark, A. E.; Marrink, S.-J. Simulation of Pore Formation in Lipid Bilayers by Mechanical Stress and Electric Fields. *J. Am. Chem. Soc.* **2003**, *125*, 6382–6383.
- (4) Tieleman, D. P. The Molecular Basis for Electroporation. *BMC Biochem.* **2004**, *5*, 10.
- (5) Gurtovenko, A. A.; Anwar, J.; Vattulainen, I. Defect-Mediated Trafficking across Cell Membranes: Insights from In Silico Modeling. *Chem. Rev.* **2010**, *110*, 6077–6103.
- (6) Teissie, J. Electroporation of the Cell Membrane. *Methods Mol. Biol.* **2014**, *1121*, 25–46.
- (7) Weaver, J. C. Electroporation - General Phenomenon for Manipulating Cells and Tissues. *J. Cell. Biochem.* **1993**, *51*, 426–435.
- (8) Frey, W.; White, J. A.; Price, R. O.; Blackmore, P. F.; Joshi, R. P.; Nuccitelli, R.; Beebe, S. J.; Schoenbach, K. H.; Kolb, J. F. Plasma Membrane Voltage Changes during Nanosecond Pulsed Electric Field Exposure. *Biophys. J.* **2006**, *90*, 3608–3615.
- (9) Gowrishankar, T. R.; Esser, A. T.; Vasilkoski, Z.; Smith, K. C.; Weaver, J. C. Microdosimetry for Conventional and Supra-electroporation in Cells with Organelles. *Biochem. Biophys. Res. Commun.* **2006**, *341*, 1266–1276.
- (10) Tarek, M. Membrane Electroporation: A Molecular Dynamics Simulation. *Biophys. J.* **2005**, *88*, 4045–4053.
- (11) Ziegler, M. J.; Vernier, P. T. Interface Water Dynamics and Porating Electric Fields for Phospholipid Bilayers. *J. Phys. Chem. B* **2008**, *112*, 13588–13596.
- (12) Böckmann, R. A.; de Groot, B. L.; Kakorin, S.; Neumann, E.; Grubmüller, H. Kinetics, Statistics, and Energetics of Lipid Membrane Electroporation Studied by Molecular Dynamics Simulations. *Biophys. J.* **2008**, *95*, 1837–1850.
- (13) Gurtovenko, A. A.; Vattulainen, I. Pore Formation Coupled to Ion Transport through Lipid Membranes as Induced by Transmembrane Ionic Charge Imbalance: Atomistic Molecular Dynamics Study. *J. Am. Chem. Soc.* **2005**, *127*, 17570–17571.
- (14) Kandasamy, S. K.; Larson, R. G. Cation and Anion Transport through Hydrophilic Pores in Lipid Bilayers. *J. Chem. Phys.* **2006**, *125*, 074901.
- (15) Gurtovenko, A. A.; Vattulainen, I. Ion Leakage Through Transient Water Pores in Protein-Free Lipid Membranes Driven by Transmembrane Ionic Charge Imbalance. *Biophys. J.* **2007**, *92*, 1878–1890.
- (16) Vernier, P. T.; Ziegler, M. J.; Sun, Y.; Gundersen, M. A.; Tieleman, D. P. Nanopore-Facilitated, Voltage-Driven Phosphatidylserine Translocation in Lipid Bilayers - in Cells and in silico. *Phys. Biol.* **2006**, *3*, 233–247.
- (17) Delemotte, L.; Dehez, F.; Treptow, W.; Tarek, M. Modeling Membranes under a Transmembrane Potential. *J. Phys. Chem. B* **2008**, *112*, 5547–5550.
- (18) Delemotte, L.; Tarek, M. Molecular Dynamics Simulations of Lipid Membrane Electroporation. *J. Membr. Biol.* **2012**, *245*, 531–543.
- (19) Kramar, P.; Delemotte, L.; Lebar, A. M.; Kotulska, M.; Tarek, M.; Miklavcic, D. Molecular-Level Characterization of Lipid Membrane Electroporation using Linearly Rising Current. *J. Membr. Biol.* **2012**, *245*, 651–659.
- (20) Tokman, M.; Lee, J. H.; Levine, Z. A.; Ho, M. C.; Colvin, M. E.; Vernier, P. T. Electric Field-Driven Water Dipoles: Nanoscale Architecture of Electroporation. *PLoS One* **2013**, *8*, e61111.
- (21) Ho, M. C.; Casciola, M.; Levine, Z. A.; Vernier, P. T. Molecular Dynamics Simulations of Ion Conductance in Field-Stabilized Nanoscale Lipid Electropores. *J. Phys. Chem. B* **2013**, *117*, 11633–11640.
- (22) Breton, M.; Delemotte, L.; Silve, A.; Mir, L. M.; Tarek, M. Transport of siRNA through Lipid Membranes Driven by Nanosecond Electric Pulses: An Experimental and Computational Study. *J. Am. Chem. Soc.* **2012**, *134*, 13938–13941.
- (23) Fernandez, M. L.; Risk, M.; Reigada, R.; Vernier, P. T. Size-Controlled Nanopores in Lipid Membranes with Stabilizing Electric Fields. *Biochem. Biophys. Res. Commun.* **2012**, *423*, 325–330.
- (24) Fernandez, M. L.; Marshall, G.; Sagues, F.; Reigada, R. Structural and Kinetic Molecular Dynamics Study of Electroporation in Cholesterol-Containing Bilayer. *J. Phys. Chem. B* **2010**, *114*, 6855–6865.
- (25) Levine, Z. A.; Vernier, P. T. Calcium and Phosphatidylserine Inhibit Lipid Electropore Formation and Reduce Pore Lifetime. *J. Membr. Biol.* **2012**, *245*, 599–610.
- (26) Casciola, M.; Bonhenry, D.; Liberti, M.; Apollonio, F.; Tarek, M. A Molecular Dynamic Study of Cholesterol Rich Lipid Membranes: Comparison of Electroporation Protocols. *Bioelectrochemistry* **2014**, in press.
- (27) Polak, A.; Tarek, M.; Tomsic, M.; Valant, J.; Ulrih, N. P.; Jamnik, A.; Kramar, P.; Miklavcic, D. Electroporation of Archaeal Lipid Membranes Using MD Simulations. *Bioelectrochemistry* **2014**, in press.
- (28) Reigada, R. Electroporation of Heterogeneous Lipid Membranes. *Biochim. Biophys. Acta* **2014**, *1838*, 814–821.
- (29) Gennis, R. B. *Biomembranes: Molecular Structure and Function*; Springer-Verlag: New York, 1989.
- (30) Zachowski, A. Phospholipids in Animal Eukaryotic Membranes: Transverse Asymmetry and Movement. *Biochem. J.* **1993**, *294*, 1–14.
- (31) Manno, S.; Takakuwa, Y.; Mohandas, N. Identification of a Functional Role for Lipid Asymmetry in Biological Membranes: Phosphatidylserine-Skeletal Protein Interactions Modulate Membrane Stability. *Proc. Natl. Acad. Sci. U.S.A.* **2002**, *99*, 1943–1948.
- (32) Balasubramanian, K.; Schroit, A. J. Aminophospholipid Asymmetry: A Matter of Life and Death. *Annu. Rev. Physiol.* **2003**, *65*, 701–734.
- (33) Vernier, P. T.; Ziegler, M. J.; Sun, Y.; Chang, W. V.; Gundersen, M. A.; Tieleman, D. P. Nanopore Formation and Phosphatidylserine Externalization in a Phospholipid Bilayer at High Transmembrane Potential. *J. Am. Chem. Soc.* **2006**, *128*, 6288–6289.
- (34) Piggot, T. J.; Holdbrook, D. A.; Khalid, S. Electroporation of the E. coli and S. Aureus Membranes: Molecular Dynamics Simulations of Complex Bacterial Membranes. *J. Phys. Chem. B* **2011**, *115*, 13381–13388.
- (35) Gurtovenko, A. A.; Vattulainen, I. Effect of NaCl and KCl on Phosphatidylcholine and Phosphatidylethanolamine Lipid Membranes: Insight from Atomic-Scale Simulations for Understanding Salt-Induced Effects in the Plasma Membrane. *J. Phys. Chem. B* **2008**, *112*, 1953–1962.
- (36) Gurtovenko, A. A.; Vattulainen, I. Lipid Transmembrane Asymmetry and Intrinsic Membrane Potential: Two Sides of the Same Coin. *J. Am. Chem. Soc.* **2007**, *129*, 5358–5359.
- (37) Gurtovenko, A. A.; Vattulainen, I. Calculation of the Electrostatic Potential of Lipid Bilayers from Molecular Dynamics Simulations: Methodological Issues. *J. Chem. Phys.* **2009**, *130*, 215107.
- (38) Gurtovenko, A. A.; Vattulainen, I. Intrinsic Potential of Cell Membranes: Opposite Effects of Lipid Transmembrane Asymmetry and Asymmetric Salt Ion Distribution. *J. Phys. Chem. B* **2009**, *113*, 7194–7198.

(39) Berger, O.; Edholm, O.; Jahnig, F. Molecular Dynamics Simulations of a Fluid Bilayer of Dipalmitoylphosphatidylcholine at Full Hydration, Constant Pressure, and Constant Temperature. *Biophys. J.* **1997**, *72*, 2002–2013.

(40) Berendsen, H. J. C.; Postma, J. P. M.; van Gunsteren, W. F.; Hermans, J. Interaction Models for Water in Relation to Protein Hydration. In *Intermolecular Forces*; Pullman, B., Ed.; Reidel: Dordrecht, The Netherlands, 1981; pp 331–342.

(41) Essman, U.; Perera, L.; Berkowitz, M. L.; Darden, T.; Lee, H.; Pedersen, L. G. A Smooth Particle Mesh Ewald Method. *J. Chem. Phys.* **1995**, *103*, 8577–8592.

(42) Bussi, G.; Donadio, D.; Parrinello, M. Canonical Sampling through Velocity Rescaling. *J. Chem. Phys.* **2007**, *126*, 014101.

(43) Parrinello, M.; Rahman, A. Polymorphic Transitions in Single Crystals: A New Molecular Dynamics Method. *J. Appl. Phys.* **1981**, *52*, 7182–7190.

(44) Lindahl, E.; Hess, B.; van der Spoel, D. GROMACS 3.0: A Package for Molecular Simulation and Trajectory Analysis. *J. Mol. Model.* **2001**, *7*, 306–317.

(45) Hess, B.; Kutzner, C.; van der Spoel, D.; Lindahl, E. GROMACS 4: Algorithms for Highly Efficient, Load-Balanced, and Scalable Molecular Simulation. *J. Chem. Theory Comput.* **2008**, *4*, 435–447.

(46) Vanegas, J. M.; Torres-Sanchez, A.; Arroyo, M. Importance of Force Decomposition for Local Stress Calculations in Biomembrane Molecular Simulations. *J. Chem. Theory Comput.* **2014**, *10*, 691–702.

(47) Ollila, O. H. S.; Risselada, H. J.; Louhivuori, M.; Lindahl, E.; Vattulainen, I.; Marrink, S. J. 3D Pressure Field in Lipid Membranes and Membrane-Protein Complexes. *Phys. Rev. Lett.* **2009**, *102*, 078101.

(48) McIntosh, T. J. Hydration Properties of Lamellar and Non-lamellar Phases of Phosphatidylcholine and Phosphatidylethanolamine. *Chem. Phys. Lipids* **1996**, *81*, 117–131.

(49) Roux, B. The Membrane Potential and its Representation by a Constant Electric Field in Computer Simulations. *Biophys. J.* **2008**, *95*, 4205–4216.

(50) Gumbart, J.; Khalili-Araghi, F.; Sotomayor, M.; Roux, B. Constant Electric Field Simulations of the Membrane Potential Illustrated with Simple Systems. *Biochim. Biophys. Acta* **2012**, *1818*, 294–302.

(51) Jensen, M. O.; Jogini, V.; Eastwood, M. P.; Shaw, D. E. Atomic-Level Simulation of Current-Voltage Relationships in Single-File Ion Channels. *J. Gen. Physiol.* **2013**, *141*, 619–632.

(52) Ollila, S. Lateral Pressure in Lipid Membranes and Its Role in Function of Membrane Proteins. Ph.D. Thesis, Tampere University of Technology: Tampere, Finland, 2010.

(53) Dehez, F.; Delemotte, L.; Kramar, P.; Miklavcic, D.; Tarek, M. Evidence of Conducting Hydrophobic Nanopores Across Membranes in Response to an Electric Field. *J. Phys. Chem. C* **2014**, *118*, 6752–6757.

(54) Polak, A.; Bonhenry, D.; Dehez, F.; Kramar, P.; M. Tarek, D. M. On the Electroporation Thresholds of Lipid Bilayers: Molecular Dynamics Simulation Investigations. *J. Membr. Biol.* **2013**, *246*, 843–850.

(55) Zeira, M.; Tosi, P.-F.; Mouneimne, Y.; Lazarte, J.; Sneed, L.; Volsky, D. J.; Nicolau, C. Full-length CD4 Electro-inserted in the Erythrocyte Membrane as a Long-lived Inhibitor of Infection by Human Immunodeficiency Virus. *Proc. Natl. Acad. Sci. U.S.A.* **1991**, *88*, 4409–4413.

(56) Elouagari, K.; Gabriel, B.; Benoist, H.; Teissie, J. Electric Field-Mediated Glycophorin Insertion in Cell-Membrane is a Localized Event. *Biochim. Biophys. Acta* **1993**, *1151*, 105–109.

(57) Mouneimne, Y.; Tosi, P.-F.; Gazitt, Y.; Nicolau, C. Electro-Insertion of Xeno-Glycophorin into the Red Blood Cell Membrane. *Biochem. Biophys. Res. Commun.* **1989**, *159*, 34–40.

(58) Sahay, G.; Alakhova, D. Y.; Kabanov, A. V. Endocytosis of Nanomedicines. *J. Controlled Release* **2010**, *145*, 182–195.